$LiNbO_3:Er^{3+}$ crystal as material for radiation-balanced lasing in infrared region

G. DEMIRKHANYAN[1,2], N. KOKANYAN[3], N. BABAJANYAN[1], E. KOKANYAN[1,2,*]
[1]*Department of Physics and it's Teaching Methods, Kh. Abovyan Armenian State Pedagogical University, 0010 Yerevan, Armenia*
[2]*Institute for Physical Research, National Academy of Sciences of Armenia, Ashtarak-2, 0204, Armenia*
[3]*Chaire Photonique, Laboratoire Matériaux Optiques Photonique et Systèmes (LMOPS), Centrale Supélec, F-57070, Metz, France*

Based on an analysis of the absorption and emission cross-section spectra of the 1%Er^{3+}: $LiNbO_3$ crystal in the spectral range 1450–1650 nm at room temperature the parameters of radiation-balanced generation were calculated. The optimal pump wavelength (1545 nm) and the RB generation wavelength (1610.8 nm) were determined. The corresponding efficiency and gain coefficients were calculated as $F_{eff} = 2.40 \times 10^{-22} cm^2$ and $F_{gain} = 4.62 \times 10^{-22} cm^2$, respectively.

(Received July 7, 2025; accepted February 4, 2026)

Keywords: Lithium niobate, Rare earth ion, Radiation-balanced lasing

1. Introduction

The concept of radiation-balanced (RB) laser operation is based on the possibility of fully (or partially) compensating the heat generated during pumping and stimulated emission by cooling via anti-Stokes fluorescence (ASF) in an active medium with a near-unity quantum yield. This concept was originally proposed in [1]. The mechanism of optical self-cooling is straightforward: when an atom absorbs a photon, it temporarily departs from thermal equilibrium with its environment and, upon returning to equilibrium, spontaneously emits a photon whose wavelength is shifted relative to that of the absorbed photon. Such processes can result in either heating (Stokes luminescence) or cooling (anti-Stokes fluorescence, ASF). Consequently, it is natural to search for active media for RB lasers among rare-earth (RE) doped materials that exhibit high ASF cooling efficiency and minimal heat generation during pumping and stimulated emission at the relevant wavelengths.

A method for estimating the parameters of solid-state RB lasers was proposed in [1–3]. In [4, 5], analytical expressions were derived for the minimum pump and laser intensities required to satisfy the RB condition, as well as for the RB generation efficiency and the maximum achievable signal gain. In [6, 7], approaches to minimizing heat generation through ASF cooling were investigated. The proposed framework enables a substantial reduction of thermal load in controlled laser systems. A comprehensive review of both experimental and theoretical progress in radiation-balanced bulk, fiber, disk, and micro-lasers is presented in [8].

Among active media for RB lasers and optical cooling, materials doped with RE ions are of particular importance, as discussed in [9–14]. Owing to the favorable spectroscopic properties of the ytterbium ion—such as a high absorption coefficient, the absence of up-conversion transitions, and low multi-phonon non-radiative losses — early research primarily focused on Yb^{3+}-doped materials [9–15]. The first a thermal bulk laser using direct diode pumping was experimentally demonstrated in a Yb^{3+}: $KGd(WO_4)_2$ crystal [13]. It should be noted, however, that due to the characteristic structure of the absorption and emission spectra of the Yb^{3+} ion, the RB generation wavelength is restricted to the range of 990–1130 nm [4, 5].

To achieve RB generation in other spectral regions, it is necessary to consider materials doped with different RE^{3+} ions. In doing so, one must take into account that, in order to ensure a luminescence quantum, yield close to unity, the analysis should be restricted to inter-Stark transitions between the ground and first excited manifolds. Thus, investigating the RB generation potential of materials doped with various RE^{3+} ions is of considerable interest. In [16], the RB laser potential of Tm^{3+}: $LiNbO_3$ crystal was investigated in the wavelength range of 1650–2000 nm.

In this work, we evaluate the potential for RB generation in Er^{3+}:$LiNbO_3$ (Er^{3+}: LN) crystals in the spectral region near 1.5 μm, corresponding to transitions between the Stark sublevels of the ground, $^4I_{15/2}$, and first excited, $^4I_{13/2}$, manifolds.

2. Materials and methods

High-purity starting materials, Nb_2O_5 (99.999%, Johnson Matthey) and Li_2CO_3 (99.995%, Merck), in powder form were used to prepare lithium niobate (LN) charges of congruent composition. Er^{3+} ions were introduced into the melt at a concentration of 1 at.% in the form of Er_2O_3 (Merck, 99.99%). Er^{3+}:LN single crystals

were grown in air by the Czochralski method using a platinum crucible with dimensions of 40 mm × 3 mm × 50 mm, heated in an RF furnace.

To obtain single-domain crystals directly during the growth process, a dc electric field corresponding to a current density of 12 A/m² was applied to the crystal–melt system. Crystal pulling was performed along the crystallographic *c*-axis at a rate of 1 mm/h, with a rotation speed of 20 rpm. The resulting Er^{3+}:LN boules, approximately 25 mm in diameter and 30 mm in length, were oriented along the principal crystallographic axes. Subsequently, samples with dimensions of 10 mm × 5 mm × 10 mm (X×Y×Z) were cut, mechanically processed, and optically polished.

The CW photoluminescence (PL) in the region of 1.5 nm was excited at 980 nm by a laser diode with a power of 10mW. The PL signal was analyzed by a monochromator equipped with a 600 grooves/mm grating and a photomultiplier tube. The PL spectrum was corrected from the response of the detector. The un-polarized photoluminescence spectrum of the $^4I_{13/2} \rightarrow {}^4I_{15/2}$ transition is given in Fig. 1.

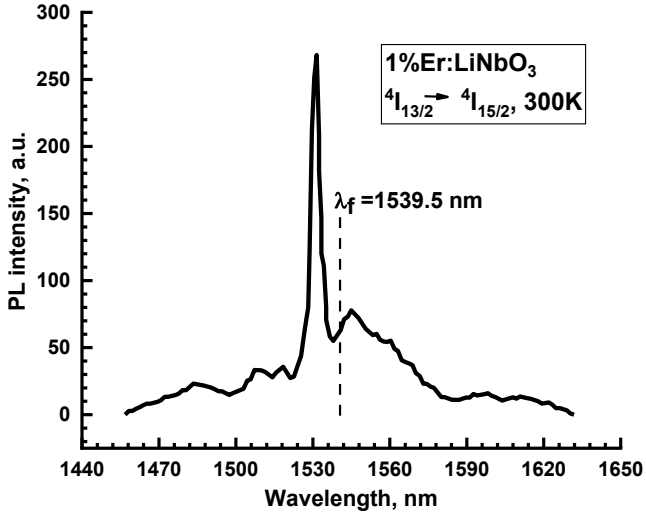

Fig. 1. Fluorescence spectrum of 1at% Er^{3+}:LN at 300K

The emission cross-section calculated using the Fuchtbauer-Ladenburg formula [17] is demonstrated in Fig. 2.

$$\sigma_{em}(\lambda) = \frac{\lambda^5}{8\pi n^2 c \tau_r} \frac{I_{em}(\lambda)}{\int \lambda I_{em}(\lambda) d\lambda} \qquad (1)$$

where n=2.2 is the refractive index [18], c is the speed of light, $\tau_r = 3\,ms$ is the radiative lifetime of the upper manifold [19].

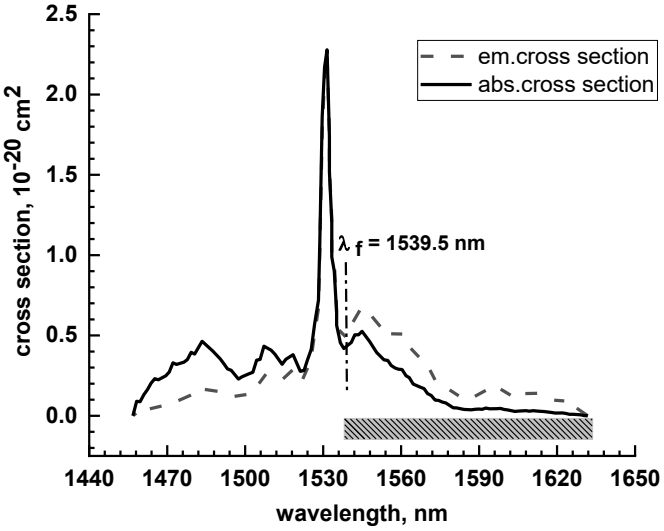

Fig. 2. Emission (dash) and absorption (solid) cross-sections of 1at% Er^{3+}:LN at 300K

Note that the RB generation parameters are sensitive to weak absorption in the long-wavelength wings. Therefore, it is preferable to determine the absorption cross-section through the emission cross-section, using the reciprocity principle [20].

$$\sigma_{abs}(\lambda) = \sigma_{em}(\lambda)\frac{Z_{up}}{Z_{gr}}\exp\left(\frac{hc-E_0\lambda}{k_B T\lambda}\right) \quad (2)$$

where E_o is the energy distance between the lower sublevels of the ground and upper manifolds, $Z_{gr,up} = \sum_i g_i exp\left[\left(E_1^{(gr,up)} - E_i^{(gr,up)}\right)/k_B T\right]$ is the statistical weights of ground and upper manifolds ($E_i^{(gr,up)}$ and g_i are energy and degeneration of i[th] sublevel of ground and upper manifolds), k_B is Boltzmann constants, T is temperature.

The necessary condition for achieving the optical cooling effect and radiation-balanced lasing is given by:

$$\lambda_f < \lambda_p < \lambda_L \quad (3)$$

where λ_p is the wavelength of the pump, λ_L is the wavelength of luminescence, and λ_f is the average wavelength of luminescence λ_F defined as:

$$\lambda_f = \int \lambda I_L(\lambda)d\lambda / \int I_L(\lambda)d\lambda \quad (4)$$

where $I_L(\lambda)$ is the luminescence intensity.

The efficiency per unit length of the optical cooling process, F_{cool}, is defined as [4]:

$$F_{cool} \equiv \frac{\eta_c(\lambda_p)}{N_t} = \sigma_{abs}(\lambda_p)\left[\frac{\lambda_p}{\lambda_f} - 1\right] \quad (5)$$

where N_t is the total active ion density and $\sigma_{abs}(\lambda_p)$ is the absorption cross-section at the pump wavelength.

The state of radiation balance is achieved when the densities of absorbed and radiated power coincide at each point of the mode volume. For this condition, the pump wavelength must satisfy equation (3). When the luminescence quantum yield is close to unity, the RB state is stable if the pump and laser intensities (I_p and I_L) satisfy the following condition [5]:

$$\frac{I_L}{I_{L_{sat}}} = \left[1 - \frac{\beta(\lambda_L)}{\beta(\lambda_P)}\left(1 + \frac{I_{P_{sat}}}{I_P}\right)\right]^{-1} \quad (6)$$

where $I_{P_{sat}}$ and $I_{L_{sat}}$ are saturation intensities defined as:

$$I_{P_{sat}} = \frac{hc}{\lambda_f \tau \sigma_{abs}(\lambda_P)} \times \eta_0 \frac{\lambda_L - \lambda_f}{\lambda_p - \lambda_f}\beta(\lambda_P) \quad (7a)$$

$$I_{L_{sat}} = \frac{hc}{\lambda_f \tau \sigma_{abs}(\lambda_L)} \times \eta_0 \beta(\lambda_L) \quad (7b)$$

Here, $\eta_0 = \frac{\lambda_p - \lambda_F}{\lambda_L - \lambda_F}$ represents the internal optical efficiency of the RB laser, τ represents the spontaneous lifetime of the active ion, h is Planck's constant, c is the speed of light, and the factor β(λ) is defined as:

$$\beta(\lambda) = \frac{\sigma_{abs}(\lambda)}{\sigma_{abs}(\lambda) + \sigma_{em}(\lambda)} = \left[1 + \frac{Z_{gr}}{Z_{up}} exp\left(\frac{E_0\lambda - hc}{k_B T\lambda}\right)\right]^{-1} \quad (8)$$

For pump intensities significantly larger than the saturation intensity, $I_P \gg I_{P_{sat}}$, the minimum value of the laser intensity can be obtained from equation (6) as:

$$I_{L_{min}} = \frac{\beta(\lambda_P)}{\beta(\lambda_P) - \beta(\lambda_L)} I_{L_{sat}} \quad (9)$$

Similarly, for large laser intensities $\left(I_L \gg I_{L_{sat}}\right)$ the minimum value of the pump intensity is given by:

$$I_{P_{min}} = \frac{\beta(\lambda_L)}{\beta(\lambda_P) - \beta(\lambda_L)} I_{P_{sat}}. \quad (10)$$

The efficiency per unit length for RB lasing is defined as:

$$F_{eff} = \sigma_{abs}(\lambda_P)\eta_0 \frac{\beta(\lambda_P) - \beta(\lambda_L)}{\beta(\lambda_P)}. \quad (11)$$

The maximum gain coefficient (g_{max}) corresponding to RB laser operation at high pumping intensities $\left(I_P \gg I_{P_{sat}}\right)$ can be expressed as [4-6]:

$$F_{gain} = \sigma_{abs}(\lambda_L)\frac{\beta(\lambda_P) - \beta(\lambda_L)}{\beta(\lambda_L)} \quad (12)$$

The optimal values of gain and efficiency are determined by choosing the optimal pump and laser wavelengths (λ_{OP} and λ_{OL}) with the lowest possible pump intensity, at which the product $F_{eff} \times F_{gain}$ reaches its maximum. [4-6].

3. Results and discussion

The absorption cross section was found in accordance with (2) using the values of the thermal distribution functions $Z_{gr} = 7.5482$ and $Z_{up} = 7.5527$, which were calculated at T=300K using the energies of the Stark sublevels of the manifolds $^4I_{13/2}$ and $^4I_{15/2}$, given in [21].

The average wavelength of luminescence, determined from the emission spectra according to equation (4) is $\lambda_f = 1539.5$ nm. We chose the pump wavelengths taking into account the condition (1), at which the absorption cross section has local maxima $\lambda_p = 1545.0$ and 1554.8 nm. In this case, taking into account the condition (1), RB generation can occur at wavelengths: 1554.8, 1560.4, 1568.8, 1596.8, and 1610.8 nm.

The values of the RB generation parameters calculated using formulas (5) - (12) are given in Table 1.

Table 1. RB lasing parameters for Er:LN

λ_p, nm	F_{cool}, 10^{-22} cm^2	λ_L, nm	η_0, %	$I_{p_{min}}$	$I_{L_{min}}$	F_{eff}	F_{gain}
				kW/cm^2		$10^{-22}cm^2$	
1545.0	0.188	1554.8	35.9	45.2	24.8	2.06	4.22
		1560.4	26.3	23.7	11.4	2.34	5.85
		1568.8	18.8	12.82	7.51	2.51	5.74
		1596.8	9.60	3.99	4.54	2.50	4.37
		1610.8	7.71	2.66	3.37	2.40	4.62
1554.8	0.343	1560.4	73.21	250.32	219.35	1.69	2.07
		1568.8	52.22	51.85	55.46	2.93	3.27

From Table 1 it can be seen that the optimal pump and emission wavelengths are $\lambda_{OP} = 1545\,nm$ and $\lambda_{OL} = 1610.8\,nm$, at which the pump intensity is minimal and the product $F_{eff} \times F_{gain}$ reaches its highest value. The corresponding figures-of-merit for RB laser are: $F_{gain} = 4.62 \times 10^{-22} cm^2$ and $F_{eff} = 2.4 \times 10^{-22} cm^2$.

The dependence of the RB radiation intensity at 1610.8nm wavelength vs the pump intensity at 1545 nm wavelength (Eq.6) is shown in Fig. 3.

To evaluate the feasibility of practical implementation of RB generation, the dependence of the output power on the pump intensity was determined for the optimal wavelengths of lasing and pumping [15]

$$\frac{I_L}{I_{L_{sat}}} = \left(1 + \frac{1}{\theta}\right)\left[\frac{\beta_p \beta_L^{-1} - \theta - 1}{1+\theta} \times \frac{I_p}{I_{p_{sat}}} - 1\right], \quad (13)$$

$$\theta = \frac{T_2 + l_i}{2\Lambda\alpha_0(\lambda_L)}.$$

Here T_2 is the coupling loss of the output mirror, l_i is the internal cavity loss, Λ is the gain medium length, and $\alpha_0(\lambda_L)$ is the absorption coefficient at the lasing wavelength.

Fig. 3 shows the dependence of the laser intensity on the pump intensity at $\lambda_{OP} = 1545\,nm$ and $\lambda_{OL} = 1610.8\,nm$. Calculations are carried out using the characteristic values of the corresponding parameters: $T_2 = 2\%$, $\Lambda = 1\text{cm}$, $l_i = 0.1\%$, 0.4%, and 0.8%, $\alpha_0(\lambda_{OL}) = N\sigma_{abs}(\lambda_{OL}) = 0.046\ cm^{-1}$ (N is the erbium concentration in LN). The crossing points represent the values of the pump and signal intensities that can satisfy the radiation-balancing condition for each corresponding cavity. Thus, as can be seen from Fig. 3, due to an additional constraint arising from the condition of radiative balance, the generation intensity does not increase linearly with increasing pump intensity, and for any RB laser there exists only a single unique pair of generation and pump intensities (I_{OP}, I_{OL}) at which the RB laser operates.

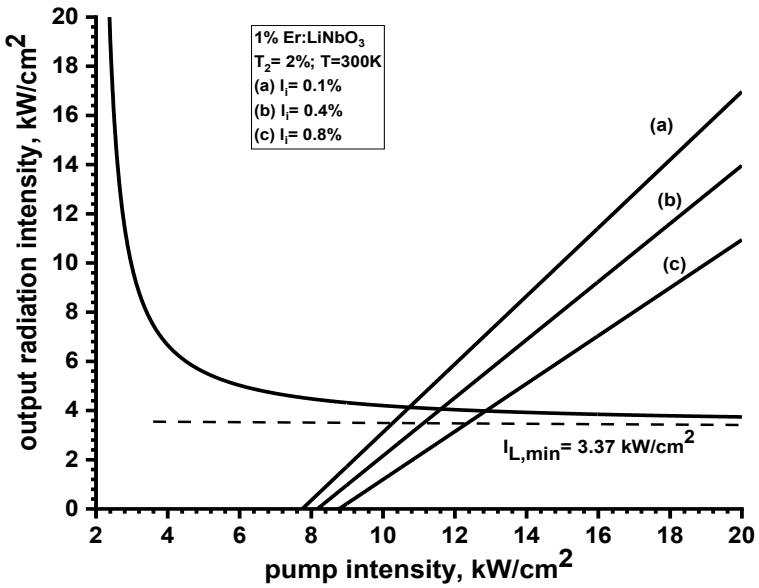

Fig. 3. The dependence of the RB lasing intensity at 1610.8 nm on pump intensity at 1545 nm and output radiation intensities at: (a) $\gamma_i = 0.1\%$, (b) $\gamma_i = 0.4\%$, (c) $\gamma_i = 0.8\%$

4. Conclusions

The optimal parameters characterizing the RB generation of 1%Er^{3+}: LN crystal are determined based on the absorption cross-section spectrum, which was found on the base of the measured fluorescence cross-section spectrum via the reciprocity method.

It is shown that, under pumping at a wavelength of 1545 nm, RB laser generation at a wavelength of 1610.8 nm is possible with a sufficiently high gain coefficient of $F_{gain} = 4.62 \times 10^{-22} cm^2$ and an efficiency of $F_{eff} = 2.4 \times 10^{-22} cm^2$. In this case, the minimum pump intensity is $I_{P_{min}} = 2.66\ kW/cm^2$, while the minimum emission intensity is $I_{L_{min}} = 3.37\ kW/cm^2$. For comparison, Table 2 presents the optimal parameters of RB generation for Yb^{3+}-doped materials. It can be seen that the Yb^{3+}:$KY(WO_4)_2$ crystal is the clear leader, demonstrating higher coefficients for both optical cooling and RB generation. However, it should be emphasized that the RB generation wavelength in Yb^{3+}-doped materials lies in the range of 1050–1070 nm, whereas for Er^{3+}: LN the RB generation wavelength is $\lambda_{OL} = 1610.8\ nm$.

To evaluate the feasibility of practical implementation of RB lasing, the dependence of the output power on the pump intensity was determined for the optimal pump and generation wavelengths (Fig. 3). It is shown that, with a 2% transmission of the output mirror and internal losses of 0.8%, RB generation at a wavelength of $\lambda_{OL} = 1610.8\ nm$ is achievable with an output intensity of $I_{out} = 3.98\ kW/cm^2$ when pumped at an intensity of $I_{pump} = 12.9\ kW/cm^2$ at a wavelength of $\lambda_{OP} = 1545\ nm$.

Table 2. The optimal parameters of RB lasing for some RE doped materials

host	λ_f	λ_{OP}	λ_{OL}	η_0	τ
	nm			%	ms
Er^{3+}:LN crystal	1539.5	1545.0	1610.8	7.7	3.0
Tm^{3+}:LN Crystal [16]	1818.6	1837	1852	55	1.1
Yb^{3+}: YAG ceramics, [11]	1018	1030.1	1049.2	39	0.90
Yb^{3+}: $KY(WO_4)$ crystal, [5]	992	1002	1041	20	0.60
Yb^{3+}: ZBLANP glass, [14]	995	1005	1024	36	1.7
Yb^{3+}: Rb_2NaYF_6 crystals, [22]	996	1011	1068	20	10.8
host	$I_{P_{min}}$	$I_{L_{min}}$	F_{cool}	F_{eff}	F_{gain}
	kW/cm^2		10^{-22} cm^2		
Er^{3+}:LN crystal	2.66	3.37	0.19	2.40	4.62
Tm^{3+}:LN Crystal [16]	38.8	26.3	0.14	0.4	0.8
Yb^{3+}: YAG ceramics, [11]	5.9	53.3	0.14	3.3	1.3
Yb^{3+}: $KY(WO_4)$ crystal, [12]	1.6	5.5	1.50	41	36
Yb^{3+}: ZBLANP glass, [14]	38	46	0.07	1.3	2.4
Yb^{3+}: Rb_2NaYF_6 crystals, [22]	1.8	17	0.02	0.25	0.34

Acknowledgments

The research was realized within the research project 26ASPU-PHYS-CON-I-1C of the Higher Education and Science Committee of MESCS RA.

References

[1] S. R. Bowman, IEEE J. Quantum Electron. **35**(1), 115 (1999)

[2] C. E. Mungan, T. R. Gosnell, Advances in Atomic, Molecular, and Optical Physics **40**, 161 (1999).

[3] C. E. Mungan, American Journal of Physics **73**(4), 315 (2005).

[4] S. R. Bowman, C. Mungan, Applied Physics B **71**, 807 (2000).

[5] S. R. Bowman, C. E. Mungan, Advanced Solid-State Lasers, H. Injeyan, U. Keller, C. Marshall (eds.), Trends in Optics and Photonics, Optical Society of America, Washington D.C., **34**, 446 (2000).

[6] S. R. Bowman, S. O'Connor, S. Biswal, N. L. Condon, A. Rosenberg, IEEE J. Quantum Electron. **46**, 1076 (2010).
[7] S. R. Bowman, Laser Cooling: Fundamental Properties and Application, G. Nemova (ed.), Pan Stanford Publishing Pte. Ltd., Singapore, 147 (2016).
[8] G. Nemova, Applied Sciences **11**(16), 7539 (2021).
[9] Z. Yang, J. Meng, A. R. Albrecht, M. Sheik-Bahae, Optics Express **27**, 1392 (2019).
[10] S. R. Bowman, S. O'Connor, S. Biswal, IEEE J. Quantum Electron. **41**(12), 1510 (2005).
[11] G. Demirkhanyan, B. Patrizi, R. Kostanyan, G. Toci, M. Vannini, A. Pirri, J. Li, Y. Feng, D. Zargaryan, Journal of Contemporary Physics (Armenian Academy of Sciences) **57**, 123 (2022).
[12] L. Cheng, L.B. Andre, D. Rytz, S. C. Rand, Optics Express **31**(7), 11994 (2023).
[13] S. R. Bowman, N. Jenkins, B. Feldman, S. O'Connor, Proc. of the Conf. on Lasers and Electro-Optics (CLEO), Long Beach, CA, USA, 32 (2002).
[14] M. Peysokhan, E. Mobini, A. Allahverdi, B. Abaie, A. Mafi, Photonics Research **8**, 202 (2020).
[15] E. Mobini Souchelmaei, Dissertation for the Degree of Doctor of Philosophy, Optical Science & Engineering, The University of New Mexico, New Mexico, 154 (2020).
[16] N. Mkhitaryan, G. Demirkhanyan, N. Kokanyan, E. Kokanyan, Armenian Journal of Physics **16**, 102 (2023).
[17] W. Krupke, IEEE J. Quantum Electron. **10**, 450 (1974).
[18] N. Polyanskiy, Scientific Data **11**, 94 (2024).
[19] L. Nunez, G. Lifante, F. Cusso, Applied Physics B **62**, 485 (1996).
[20] A. S. Yasyukevich, V. G. Shcherbitskii, V. Kisel, A. V. Mandrik, N. V. Kuleshov, Journal of Applied Spectroscopy **71**, 202 (2004).
[21] J. B. Gruber, D. K. Sardar, R. M. Yow, E. P. Kokanyan, Physical Review B **69**(19), 195103 (2004)
[22] G. Nemova, R. Kashyap, Reports on Progress in Physics **73**, 086501:1-20 (2010).

*Corresponding author: edvardkokanyan@gmail.com